

ChemComm

Accepted Manuscript



This is an *Accepted Manuscript*, which has been through the Royal Society of Chemistry peer review process and has been accepted for publication.

Accepted Manuscripts are published online shortly after acceptance, before technical editing, formatting and proof reading. Using this free service, authors can make their results available to the community, in citable form, before we publish the edited article. We will replace this *Accepted Manuscript* with the edited and formatted *Advance Article* as soon as it is available.

You can find more information about *Accepted Manuscripts* in the [Information for Authors](#).

Please note that technical editing may introduce minor changes to the text and/or graphics, which may alter content. The journal's standard [Terms & Conditions](#) and the [Ethical guidelines](#) still apply. In no event shall the Royal Society of Chemistry be held responsible for any errors or omissions in this *Accepted Manuscript* or any consequences arising from the use of any information it contains.

Selective CO₂ reduction on polycrystalline Ag electrode enhanced by anodization treatment

Received 00th January 20xx,
Accepted 00th January 20xx

Li Qin Zhou,* Chen Ling, Michael Jones and Hongfei Jia

DOI: 10.1039/x0xx00000x

www.rsc.org/

Electrochemical reduction of CO₂ to CO on polycrystalline silver (Ag) was greatly improved by a simple anodization treatment. A CO Faradaic efficiency of 92.8% was achieved at 0.50 V of overpotential in an aqueous electrolyte. This study suggests that the enhanced performance is due to a preferred (220) orientation and a thin silver oxide layer formed by the anodization.

The atmospheric carbon dioxide concentration has been rising at an accelerating rate since the age of industrialization, which may lead to global warming and unpredictable climate changes that endanger the sustainability of human society.¹ One remedy to this grand challenge is to promote renewable carbon cycles known “artificial photosynthesis”, which uses solar energy to convert CO₂ to fuels or other chemicals.^{2,3} Electrochemical catalysis represents an effective approach to CO₂ conversion. However, further advance on the development of electrode catalysts is necessary to minimize energy loss due to the high activation energy barrier of CO₂ reduction reaction. In addition, as practical implementation of such type of processes prefers to operate in an aqueous electrolyte, electrocatalytic CO₂ reduction must compete with hydrogen evolution, which typically has fast kinetics and occurs at a lower electrode potential.^{4,5} Several potential catalysts have been identified previously for selectively reducing CO₂ in aqueous electrolytes.⁵⁻⁷ Among these catalysts, Ag is a promising material because it selectively catalyses the reduction of CO₂ to CO at room temperature.⁵⁻⁷ However, a large overpotential is usually necessary for CO₂ reduction on typical polycrystalline silver electrode, and the CO selectivity decreases substantially at low overpotentials.⁸ Hence many researchers have recently tried to develop new methods to enhance the performance of Ag electrodes at low overpotentials. Rosen et al. reported using Ag nanoparticles as an electrocatalyst in an ionic liquid electrolyte (EMIM-BF₄).⁹⁻¹¹ An electrocatalytic reduction of CO₂ to CO at a low overpotential of 170 mV was observed. Lu et al. reported a nanoporous Ag electrocatalyst with 92% selectivity under a moderate overpotential of 0.40-0.50 V.¹² The nanoporous Ag was fabricated by arc melting of Ag and Al into an alloy, followed by a two-step de-alloying process. Here we report a simple and low-cost anodization approach to modify Ag electrode, through which CO selectivity can be significantly improved at low overpotentials 0.3-0.5 V.

The anodized Ag electrodes were prepared using commercially

available Ag foil which was mechanically polished and sonicated with DI water prior to anodization. Anodization was conducted in 0.1 M aqueous NaNO₃ (neutral or pH3) with various potentials against Ag/AgCl (0.45, 0.50, 0.55, 0.60, 0.65, 0.70, and 0.90 V) and charges (3, 5, 5.5, 6, 7, and 10 coulombs). The electrolysis was conducted in 0.1 M aqueous KHCO₃ electrolyte and was terminated after the transfer of 10 coulombs of total charge. Gas phase products were analysed using gas chromatography. The experimental details for the electrode preparation, electrochemical tests and the structural analysis are described in the experimental procedures in the ESI.†

Fig. 1(a) shows the CO Faradaic efficiency (FE_{CO}) vs. overpotential for unanodized polycrystalline Ag electrode (denoted as poly-Ag) and electrode anodized at different potentials against Ag/AgCl. The poly-Ag electrode exhibited poor CO selectivity as evidenced by low FE_{CO} especially at low overpotentials. The majority of the activity was due to H₂ evolution, which was in consistent with previous reports.^{8,12} The anodized electrode, on the other hand, showed significantly improved FE_{CO}. Taking the FE_{CO} at the overpotential of 0.5 V as an example, the CO selectivity continued to increase with the anodization potential up to 0.6 V, beyond which it started to drop for electrodes anodized at larger potentials. Fig. 1(b) displays the FE_{CO} for electrodes anodized at 0.6 V with different amount of charges. The CO selectivity increased with the total amount of anodization charge up to 5.5 C, followed by a decrease of FE_{CO} for further increase in the amount of charges.

In order to provide a direct comparison of the electrocatalytic performances for different electrodes, Fig. 1(c) plots the FE_{CO} vs. current density measured at the overpotential of 0.5 V. It is clear that the anodized electrodes showed great improvement in terms of both activity (current density) and CO selectivity (FE_{CO}). The best FE_{CO} of 92.8% was achieved for Ag electrode anodized at 0.6 V potential with the total charge of 5.5 C (denoted as an-Ag hereafter). Coincidentally, this same electrode also exhibited the largest current density of 3.70 mA/cm². Compared to poly-Ag electrode (0.18 mA/cm²), the current density was 21 times higher and the FE_{CO} (4.8% for poly-Ag and 92.8% for an-Ag) was 19 times higher at this moderate overpotential.

We also examined the effects of pH of the anodization electrolytes. Fig. S1 shows the electrocatalytic performance of the electrode anodized at pH3 electrolyte at the optimized potential of 0.6 V and charge of 5.5 C. The CO Faradaic efficiency at 0.5 V overpotential was ~50%, suggesting that the neutral pH was essential to achieve the best performance for the anodized Ag electrode.

Based on these results, the electrodes anodized at 0.6 V with charge of 5.5 C in neutral NaNO₃ were selected for further characterization and CO₂ reduction studies.

Materials Research Department, Toyota Research Institute of North America (TRI-NA), 1555 Woodridge Ave., Ann Arbor, Michigan 48105, USA. E-mail: liqing.zhou@tema.toyota.com

† Electronic Supplementary Information (ESI) available: Experimental details and supporting figures. See DOI: 10.1039/x0xx00000x

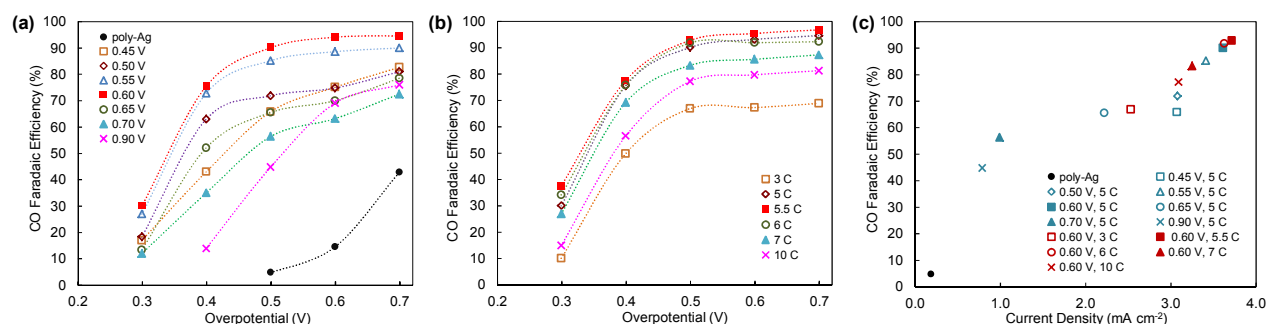


Fig. 1 Electrochemical performance of anodized Ag electrodes. (a) CO Faradaic efficiency for Ag electrodes anodized at different potentials against Ag/AgCl. The anodization charge was fixed at 5 coulombs in a neutral (pH7) 0.1 M NaNO₃ electrolyte. (b) CO Faradaic efficiency for Ag electrodes anodized at different charges. The anodization potential was fixed at 6.0 V against Ag/AgCl in a neutral 0.1 M NaNO₃ electrolyte. (c) CO Faradaic efficiency (at 0.5 V overpotential) and current density (when 10 coulombs of total charge passed through) for Ag electrodes anodized under various conditions in a neutral 0.1 M NaNO₃ electrolyte. The anodization conditions are labeled as “anodization potential, charge”.

Fig. 2 presents the current density and Faradaic efficiency under a prolonged operation of two hours for the an-Ag and poly-Ag. For the poly-Ag electrode, the current density slightly increased in the first 15 minutes and stabilized afterwards. In contrast, the an-Ag electrode recorded very stable current density without any appreciable change in the entire range of operation. Furthermore, the CO Faradaic efficiency for the an-Ag electrode was maintained above 92% throughout 2 hours of electrocatalytic process, confirming the excellent sustainability of the anodized Ag electrode.

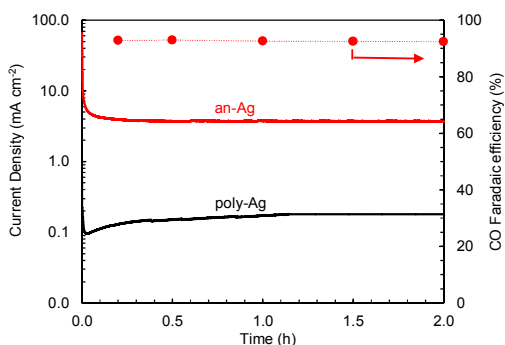


Fig. 2 Current density during a 2-hour electrocatalysis for an-Ag electrode in comparison with poly-Ag (solid lines, left axis) and CO Faradaic efficiency versus time for an-Ag electrode (dots, right axis).

A typical scanning electron microscopy (SEM) picture of the an-Ag electrode is shown in Fig. S2, in comparison with the poly-Ag. A porous surface structure was observed after anodization and the anodized layer extended to about 2 μm in thickness. The electrodes anodized with different conditions did not exhibit appreciable difference in surface morphology. Therefore we anticipated that the anodization process improved the surface area of the electrode,

which was certainly beneficial to promote the electrocatalytic activity.

The electrochemically active surface area of the an-Ag was measured (the experimental details are described in the ESI). The an-Ag showed an electrochemical surface area 5 times higher than that of the poly-Ag (Fig. S3), way less increase than the current density (21 times at 0.5 V overpotential) and CO selectivity (19 times at 0.5 V overpotential). These results indicated that more intrinsic changes to the surface structure were involved, in addition to the increase in the surface area created by the anodization.

To obtain insight into the mechanistic pathway(s) for CO₂ reduction on the surface of the anodized electrodes, Tafel analysis was performed to compare the an-Ag with the poly-Ag. The results are shown in Fig. 3. The anodized Ag has a Tafel slope of 66 mV dec⁻¹ compared with 140 mV dec⁻¹ for the unanodized counterpart. It is widely accepted that reduction of CO₂ to CO is a two-electron process.⁴ In the first step, one electron is transferred to a CO₂ molecule and forms a CO₂⁻ intermediate specie that is adsorbed on the metal surface. In the subsequent steps, the CO₂⁻ anion takes two protons and another electron to form one CO and one H₂O molecule. According to previous studies,^{7,12} the first electron transfer is the rate-determining step on unanodized polycrystalline Ag electrode, as supported by the Tafel slope of 140 mV dec⁻¹, which is close to the calculated value of 120 mV dec⁻¹.¹³ However, for the anodized Ag, the significantly lower Tafel slope of 66 mV dec⁻¹ indicates faster electron transfer and a possible change of the rate-determining step to the migration of HCO₃⁻ on the surface.¹² Tafel results further indicated that the surface structures of the anodized Ag are distinct from the unanodized Ag.

Fig. 4 (a) presents the grazing incidence X-ray diffraction (GIXRD) patterns of Ag electrodes anodized at 0.6 V for 5.5 C in pH7 and pH3. The GIXRD patterns of other samples are presented in Fig. S4. While both the unanodized and anodized electrodes show polycrystalline structures, their crystal orientations are quite different. After the anodization, the (220) peak intensity became significantly stronger. Ag (220) surface is argued to exhibit higher activity towards CO₂ reduction than (111) surface.^{7,14} We calculated the intensity ratios of (220) to (111) as an indicator of (220)

preferability for all electrodes and plotted them with respect to CO Faradaic efficiency measured at 0.5 V overpotential (Fig. 4 (b)). With the increase of (220)/(111) peak intensity ratio CO Faradaic efficiency substantially increased for the electrodes anodized in neutral electrolyte. Therefore, the improved performance of the anodized Ag electrodes was attributed to the created porous structures that selectively preserved (220) surface in the anodization process, which enhanced the activity of CO₂ reduction to CO. Mechanism for forming the preferred Ag (220) orientation by anodization is unclear and needs further study. One possible mechanism is the anisotropic electrochemical etching of different crystalline planes. In addition, a previous report on the successful fabrication of various crystallographically oriented TiO₂ nanotube arrays via anodization of Ti films on indium tin oxide glass¹⁵ supports the notion that anodization process could alter the structural orientations. We are conducting further study on this subject.

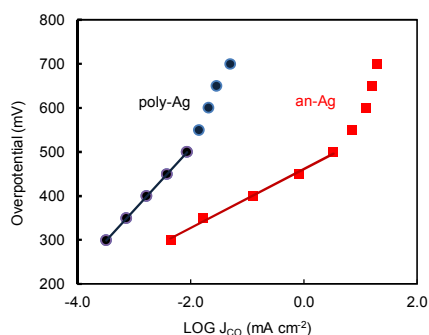


Fig. 3 Tafel plots of Ag electrode anodized at potential of 0.6 V for 5.5 coulombs of charge in neutral 0.1 M NaNO₃ electrolyte, and unanodized poly-Ag.

It is noticed that the Ag electrode anodized in pH3 electrolyte exhibits similar structural orientation with those in neutral electrolyte (Fig. 4(a)), but significantly lower selectivity (e.g., 50% vs. 92.8% at 0.5 V overpotential). This observation implied that the electrocatalytic performance is also affected by factors other than the surface orientation. X-ray photoelectron spectroscopy (XPS) analysis was conducted to provide insights on the mechanism. High resolution O 1s and Ag 3d scans for the poly-Ag and anodized samples are shown in Fig. 5. The O 1s spectrum for the poly-Ag revealed a peak with two main components, one at 531.5 eV and the other at 533.2 eV, which are usually assigned to adsorbed oxygen molecules.¹⁶⁻¹⁸ The spectrum for the pH7 anodized (at 0.6 V for 5.5 C charge) sample contained, in addition to the components at 531.5 and 533.2 eV that were observed in unanodized Ag, two lower binding energy components at 530.8 and 529.3 eV, which are related to lattice oxygen being assigned to Ag-O-Ag and Ag-O bonds, respectively.^{14,16,17} These low binding energies were not observed in the pH3 anodized (at 0.6 V for 5.5 C charge) sample. The formation of silver oxide in the pH7 anodized sample surface was also confirmed by the Ag 3d spectrum, where a shift in both the Ag 3d_{3/2} and Ag 3d_{5/2} peaks to a lower binding energy was clearly observed.¹⁸

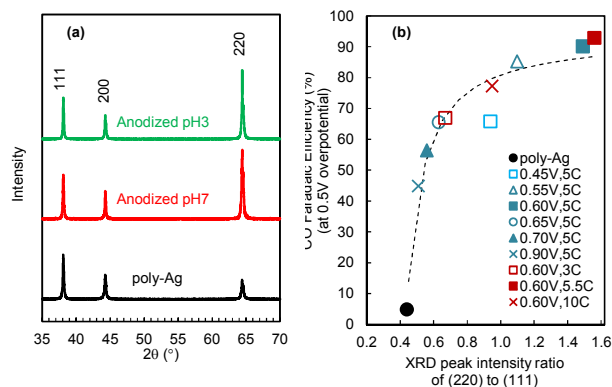


Fig. 4 (a) Grazing incidence XRD patterns of anodized (in neutral and pH3 electrolyte at potential of 0.6 V against Ag/AgCl and 5.5 coulombs of charge) and unanodized poly-Ag. The intensity was normalized to the (111) peak. (b) Correlation between CO selectivity and (220) preferability for electrodes anodized in neutral electrolyte. The XRD peak intensity ratio of (220) to (111) was used as an indicator of the preferred (220) orientation. The anodization conditions are denoted in the figure as “anodization potential, charge”.

As shown in Fig. S5, no Ag oxidation was observed after anodization at potentials lower than 0.45 V. When the anodization potential was higher than 0.7 V, Ag was further oxidized to state higher than Ag₂O, as indicated by the increase of O 1s peak at 529.3 eV and the further shift of Ag 3d_{3/2} and Ag 3d_{5/2} peaks to lower binding energies (Fig. S5(a)). On the other hand, the oxidation of Ag was not appreciably dependent on the amount of anodization charge, as shown in Fig. S5(b). These results are in fully agreement with the Pourbaix's potential-pH equilibrium diagram for the silver-water system.¹⁹ For anodization in neutral solution, Ag started to get oxidized to Ag₂O when the potential was raised to 0.6 V, and was further oxidized to AgO with higher potential. As for low pH3 anodization, no Ag oxide formed.

It is important to point out that before the electrochemical tests of each electrode, 5 cycles of cyclic voltammetry (over an applied potential range of -0.5 to -1.5 V vs. Ag/AgCl) were run to condition the electrodes (see ESI for experimental details). The XPS of the conditioned samples are shown in Fig. S6. No silver oxide was found on the surface of any of the samples, indicating a complete reduction of the silver oxide layer after the conditioning electrocatalysis.

These results suggested that the formation of a thin silver oxide layer on the surface of Ag electrode and subsequent reduction of this oxide layer plays a critical role in promoting CO₂ reduction. Previous studies demonstrated that the oxidation and subsequent electrochemical reduction of metals such as Cu, Au and Sn greatly improved their catalytic performance.²⁰⁻²⁵ This work indicated that silver oxide formed in anodized Ag likely played a similar role as the Cu, Au and Sn metallic catalysts.

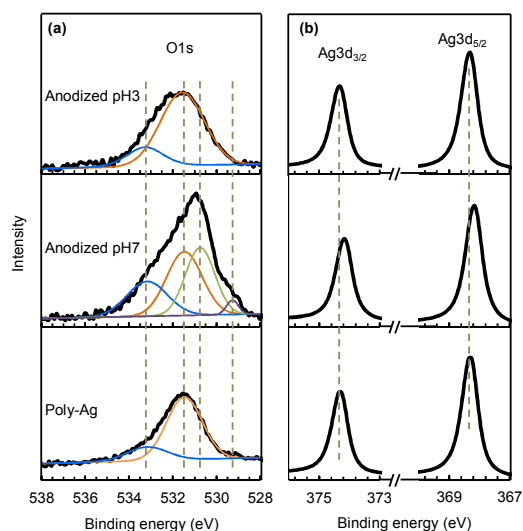


Fig. 5 O 1s (a) and Ag 3d (b) XPS spectra of anodized Ag in neutral and pH3 electrolytes (at 0.6 V for 5.5 C charge) in comparison with poly-Ag. The deconvolution of the O 1s spectrum is also illustrated. In (b), the intensity was normalized to Ag 3d_{5/2} peak.

In this communication, we demonstrated a simple and effective approach via anodization to improve CO₂ reduction activity and CO selectivity on polycrystalline Ag electrode. Under a moderate overpotential of 0.5 V, 92.8% Faradaic efficiency was achieved using the anodized Ag electrodes. Microstructural and electronic structure analyses revealed that the high activity and selectivity were closely related to the preferred Ag (220) orientation and the formation of silver oxide by anodization.

Notes and references

- N. S. Lewis and D. G. Nocera, *PNAS*, 2006, **103**, 15729.
- L. Hammarstrom and S. Hammes-Schiffer, *Acc. Chem. Res.*, 2009, **42**, 1859.
- R. Angamuthu, P. Byers, M. Lutz, A. L. Spek and E. Bouwman, *Science*, 2010, **327**, 313.
- Y. -J. Zhang, V. Sethuraman, R. Michalsky and A. A. Peterson, *ACS Catal.*, 2014, **4**, 3742.
- Y. Hori, *Modern Aspects of Electrochemistry*, Vol. 42, Springer, New York, 2008.
- K. P. Kuhl, E. R. Cave, D. N. Abram and T. F. Jaramillo, *Energy Environ. Sci.*, 2012, **5**, 7050.
- Q. Lu, J. Rosen and F. Jiao, *ChemCatChem*, 2015, **7**, 38.
- T. Hatsukade, K. P. Kuhl, E. R. Cave, D. N. Abram, and T. F. Jaramillo, *Phys. Chem. Chem. Phys.*, 2014, **16**, 13814.
- B. A. Rosen, A. Salehi-Khojin, M. R. Thorson, W. Zhu, D. T. Whipple, P. J. A. Kenis and R. I. Masel, *Science*, 2011, **334**, 643.
- B. A. Rosen, W. Zhu, G. Kaul, A. Salehi-Khojin and R. I. Masel, *J. Electrochem. Soc.*, 2013, **160**, H138.
- A. Salehi-Khojin, H.-R. M. Jhong, B. A. Rosen, W. Zhu, S. Ma, P. J. A. Kenis and R. I. Masel, *J. Phys. Chem. C*, 2013, **117**, 1627.
- Q. Lu, J. Rosen, Y. Zhou, G. S. Hutchings, Y. C. Kimmel, J. G. Chen and F. Jiao, *Nat. Commun.*, 2014, **5**, 3242.
- E. Gileadi, *Electrode Kinetics for Chemists, Engineers, and Materials Scientists*, Wiley-VCH, 1993.
- N. Hoshi, M. Kato and Y. Hori, *J. Electroanal. Chem.*, 1997, **440**, 283.
- L. Wang, Y. Wang, Y. Yang, X. Wen, H. Xiang and Y. Li, *RSC Adv.*, 2015, **5**, 41120.
- P. Prieto, V. Nistor, K. Nouneh, M. Oyama, M. Abd-Lefdil and R. Diaz, *Appl. Surf. Sci.*, 2012, **258**, 8807.
- A. I. Boronin, V. I. Bukhtiyarov, A. L. Vishnevskii, G. K. Borekov and V. I. Savchenko, *Surf. Sci.*, 1988, **201**, 195.
- A. I. Boronin, S. V. Koscheev and G. M. Zhidomirov, *J. Electron. Spectrosc. Relat. Phenom.*, 1998, **96**, 43.
- M. Pourbaix, *Atlas of Electrochemical Equilibria in Aqueous Solutions*, National Association of Corrosion Engineers, Houston, 1974.
- K. W. Frese, *J. Electrochem. Soc.*, 1991, **138**, 3338.
- M. Le, M. Ren, Z. Zhang, P. T. Sprunger, R. L. Kurtz and J. C. Flake, *J. Electrochem. Soc.*, 2011, **158**, E45.
- C. W. Li and M. W. Kanan, *J. Am. Chem. Soc.*, 2012, **134**, 7231.
- C. W. Li, J. Ciston and M. W. Kanan, *Nature*, 2014, **508**, 504.
- Y. Chen, C. W. Li and M. W. Kanan, *J. Am. Chem. Soc.*, 2012, **134**, 19969.
- S. Zhang, P. Kang and T. J. Meyer, *J. Am. Chem. Soc.*, 2014, **136**, 1734.